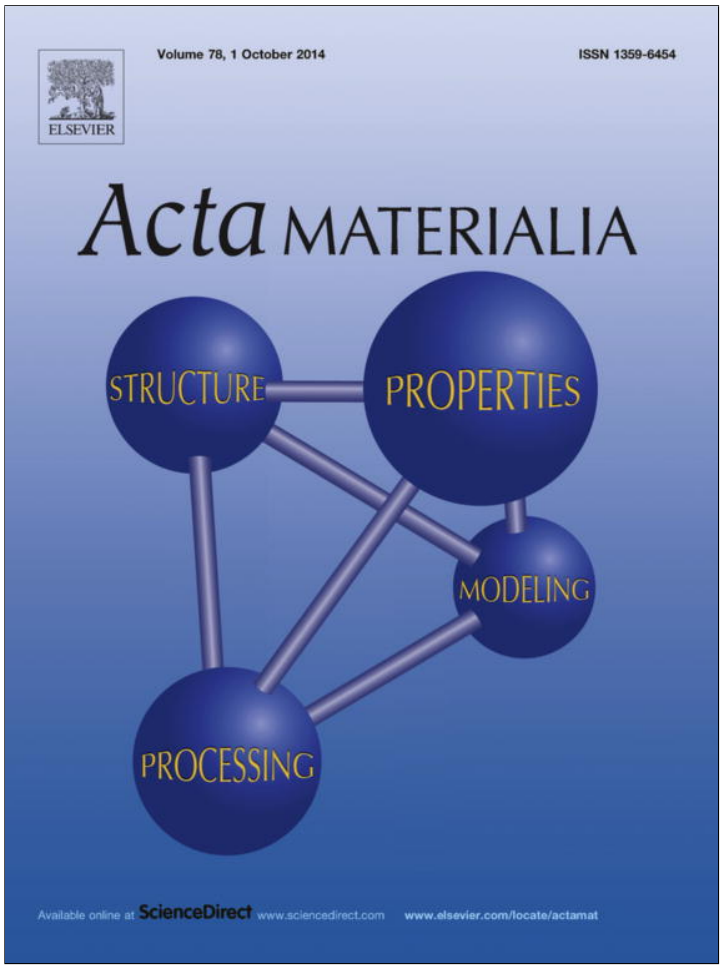

Available online at www.sciencedirect.com

ScienceDirect

Acta Materialia 78 (2014) 301–313

Acta MATERIALIA

www.elsevier.com/locate/actamat

Role of cell regularity and relative density on elastoplastic compression response of 3-D open-cell foam core sandwich structure generated using Voronoi diagrams

Oscar E. Sotomayor, Hareesh V. Tippur *

Department of Mechanical Engineering, Auburn University, AL 36849, USA

Received 21 May 2014; received in revised form 10 June 2014; accepted 20 June 2014
Available online 26 July 2014

Abstract

The Voronoi tessellation technique in a 3-D space is used for modeling the structural foam core used in sandwich configurations. The procedure involves stochastic generation of nuclei in a control volume. The level of randomness of the microstructure is controlled with a simple sequential inhibition (SSI) process and quantified using a regularity parameter. The influence of the cell regularity on the compression response of open-cell microstructures is studied in the elastic and plastic deformation regimes. Additionally, the effect of relative density is analyzed for different regularities and results are compared with available analytical and semi-empirical models. The low probability of generating highly regular structures using the SSI process has led to the development of a perturbation approach to complement the SSI methodology. Models for estimating elastoplastic properties based on the density of the foam and the regularity parameter are presented. Simulations suggest a monotonic and direct relationship between mechanical properties and the regularity parameter for the entire range of strains considered.

Keywords: Cellular solids; Voronoi diagrams; Virtual design; Cell regularity; Compression

1. Introduction

Open-cell metallic or polymeric foams are man-made cellular solids that emulate microstructures commonly observed in nature [11]. They offer low relative density and have interconnected network of struts and/or faces resulting in high strength-to-weight ratios and energy absorption characteristics suitable for aerospace, automotive, military and other applications. An overview of the processing methods, characteristics and applications of the resulting foams can be found in Ashby et al. [2] and Banhart [3]. Irrespective of the method used for producing these foams, the mechanism responsible for the intricate morphology of open-cell configurations can be linked to a process involving expansion of bubbles in a 3-D space [2]. As a consequence, each foam specimen has a unique, non-repeatable and non-periodic cellular structure/morphology. It is important to recognize that in the currently used methods of foam production the initial conditions are imposed with very limited control over the final morphology of the resulting foam. The relative density ($\bar{\rho}$) (defined as a ratio between the density of the cellular solid to the density of the bulk material (ρ^*/ρ_s)) and the average cell size are the two morphological characteristics that are controlled using methods identified in Ashby et al. [2]. On the other hand, the cross-sectional shape of struts, the polydispersity of cells, the regularity of cells and the macroscopic shape of the resulting foam are normally consequences of physical laws inherent to the pro-

* Corresponding author. Tel.: +1 334 844 3327.
E-mail address: tippuhv@auburn.edu (H.V. Tippur).

http://dx.doi.org/10.1016/j.actamat.2014.06.051
1359-6454/

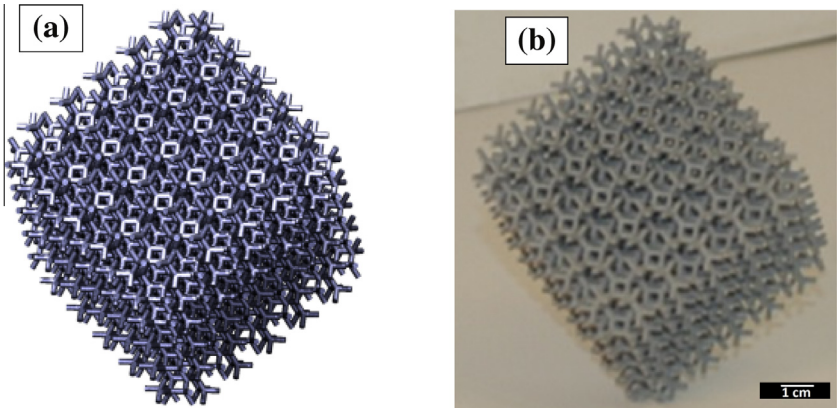

Fig. 1. Voronoi foam with 341 cells from a regular body-centered arrangement of points, produced with a laser-sintering technology: (a) virtual model; (b) 3-D printed specimen.

duction method used and are essentially uncontrolled during the foam production processes using conventional methods.

The relative density is the dominant parameter that influences the mechanical behavior of structural foams. Studies regarding the influence of relative density on the elastic response of foams are widely available in the literature [11,38,43]. For instance, by making use of a regular tetrakaidecahedron representation, Zhu et al. [43] derived analytical expressions for estimating the elastic properties of foams as a function of the relative density. Another model for estimating the elastic properties of open-cell foams has been proposed by Warren and Kraynik [38]. In their approach a unit structure formed by struts joining the centroid of a tetrahedron with its vertices was used in order to maintain the 109.5° edge connectivity. The cell size is the other morphological parameter that can be controlled during foam production. Experiments, however, have shown that the cell size has little effect on the compression response of open-cell foams [19,29]. The remaining characteristics have received less attention, possibly due to the technological shortcomings to control them during traditional production processes. However, with the rapid advancement in additive manufacturing methods and their widespread availability, control over the cross-sectional shape of struts/ligaments, cell regularity, polydispersity and macroscopic shape can all be readily tuned and hence need to be studied carefully. For instance, Fig. 1 shows an example of a regular open-cell foam generated in a virtual 3-D space along with the real model produced using an additive manufacturing technique. Specifically, the model was produced using a laser-sintering technique in which a mixture of polylaurinlactam powder and aluminum grit was used.[1] Thus, the restrictions normally imposed by conventional production techniques are largely eliminated with continued progress in printable materials, and the morphology of the foam can be fully controlled within the present-day technological limits on layer thickness, type of base material and microfeatures.

Attempts to computationally investigate foams using finite-element (FE) methods range from homogenization approaches [21] to the use of repeating unit cells or cell clusters [14,15,16,23,25]. An efficient approach to model open-cell metal foams is by using a planar-faced isotropic tetrakaidecahedron, an approximation of the minimal space dividing cell proposed by Sir William Thompson (Lord Kelvin) [37]. Nevertheless, a regular tetrakaidecahedron cannot accurately represent the structure of open-cell metal foams [31,39]. A different technique to realistically construct the geometry of foams is to create 3-D volumes using tomographic information of real foams. However, the spatial resolution, the size of data set generated and the cost of hardware/software can all be issues to address in its application to real-world problems [13,24]. In an effort to better represent the morphology of honeycombs (2-D) and foams (3-D) and simulate their mechanical response in an efficient way, the Voronoi tessellation technique in 2-D [7,34,36] and 3-D [9,10,18,33] in conjunction with FE methods has been applied. That is, to represent foams, normally a pattern of points is generated to create Voronoi diagrams that closely resemble the morphology of real foams. To date, much attention has been paid to the influence of relative density and cell size on the mechanical response of foams. In addition, there is a lack of research on the role of cell regularity on the mechanical performance of structural foams. In fact, the regularity parameter is somewhat rarely identified when the Voronoi tessellation technique is applied to represent foams virtually even though it has a rather profound effect on the final topology of honeycombs (2-D) or foams (3-D). The effect of regularity on the compression response of Voronoi honeycombs with a linear elastic base material is presented in Zhu et al. [42], [44]. In 3-D, Zhu et al. [41] studied the compression response of low-density Voronoi foams with an

[1] In the laser-sintering technique, thin layers of the powder material are deposited onto a planar platform. Subsequently, a laser beam fuses the powder in regions defined by a computer-aided design model. The platform is then lowered and another layer of powder is applied. The process is repeated until the final product is created.

elastic base material. A different approach to study the effect of regularity on the compression response of structural foams is presented by Luxner et al. [26]. In their approach a random perturbation of the location of the vertices of regular tetrakaidecahedron and cubic foams is introduced. As a consequence, random but relatively regular configurations are generated. Interestingly, Zhu et al. [41] and Luxner et al. [26] differ in their conclusion about the effect of randomness on the elastic response of foams although the studies are in different ranges of relative density. Further, the differences can be possibly explained due to the different techniques used by these investigators for constructing their geometries. In Luxner et al. [26] approach, all the cells have 14 faces and the possibility of creation of re-entrant cells cannot be excluded.

In this context, the focus of this work is on studying the effect of cell regularity on the compression response of foam core materials loaded in a sandwich configuration over a wide range of regularities from fully random to highly regular Voronoi foams using a FE method. Unlike previous works which have studied the effect of regularity on the compression response of Voronoi honeycombs and foams by modeling the base material as a linear elastic solid, here it is modeled with an elastoplastic response. Additionally, the influence of the face sheets on the overall response of the model is analyzed in the Appendix. The effect of relative density on the compression response of foams is also studied and results are compared with analytical and empirical counterparts available in the literature. Open-cell aluminum foams with Al-6101-T6 base material and 40 pores per inch have been used as an initial target of simulations based on commercially available open-cell foams. The results have been subsequently normalized to generalize them to other structural foams.

2. Solid modeling

2.1. Voronoi diagrams

In the case of open-cell foams, by having a set of n nuclei to represent the location of the centers of bubbles growing in a m-dimensional Euclidean space, a Voronoi tessellation technique can be used to link all the points in that space with the nearest nucleus [22,28,30], generating n regions that form the Voronoi diagram. In this work, such a division of space has been implemented in Matlab® using the Qhull algorithm [4].[2] The Voronoi diagram represents the limiting case of growing bubbles in space under the assumption that (i) bubbles nucleate simultaneously in a determinate region of space, (ii) bubbles stay in fixed positions during growth, (iii) the rate of growth is constant in all directions, and (iv) the growth is interrupted when a bubble touches an adjacent bubble [5,35,36]. As the Voronoi diagram is unique for a given set of nuclei, the shape of the Voronoi diagram can be controlled by generating a different arrangement (or distribution) of nuclei [22,28,30]. For the case of monodispersed nuclei, a fully regular pattern of points generates regular Voronoi diagrams whereas a similar assertion can be made for the irregular case as well. Natural and conventional foams are neither fully irregular nor fully regular. Their cellular morphology is somewhere in between these two limits.

[2] Initially developed at the Geometry Center of the University of Minnesota, Minneapolis, MN.

2.2. Regularity parameter

A pseudo-random arrangement of points in a space can be generated using a Poisson probability distribution if (i) the points are generated independently from the previous ones, (ii) the probability of a nucleus being generated in a region of space is proportional to the size of the region, and (iii) the probability of any two nuclei generated at the same location is negligible [27,30]. As mentioned previously, a fully random Voronoi foam generated with a Poisson probability distribution does not fully represent the morphological characteristics observed in foams [11]. For example, the range of cell sizes generated with a fully random arrangement of nuclei is too broad when compared to that in real foams. For that reason, it is necessary to increase the regularity of the nuclei. This is typically accomplished by eliminating points that are closer than a certain distance, denoted by the so-called distance of inhibition (s). In this work, a simple sequential inhibition (SSI) algorithm available in Matlab® and proposed by Martinez and Martinez [27] was used to accomplish the task. In a SSI process, a set of points are randomly generated one at a time based on Poisson probability distribution. The distance of a point thus generated relative to the previous ones is checked during each iteration. A point is eliminated if its distance from the previous ones is less than a prescribed distance of inhibition (s). Increasing the distance of inhibition increases the regularity of the arrangement of nuclei. However, the distance of inhibition has a maximum value that corresponds to the distance in a fully ordered (regular) arrangement of points. The maximum possible value of the distance of inhibition is a function of the size of the space (region) and the number of points to be generated. Zhu et al. [41] have presented a formula for calculating the maximum distance of inhibition (r) in 3-D as:

$$r = \frac{\sqrt{6}}{2}\left(\sqrt[3]{\frac{V}{\sqrt{2}n}}\right). \tag{1}$$

In the above equation, V is the control volume within which n nuclei are located. Hence, the regularity parameter can be quantified with s or using a ratio of s to the maximum value r (see [41,42] and references therein) as:

$$\delta = \frac{s}{r}. \tag{2}$$

In the present work, δ will be referred to as the regularity parameter or simply the "regularity". Fig. 2 illustrates an example of the effect of increasing the regularity parameter

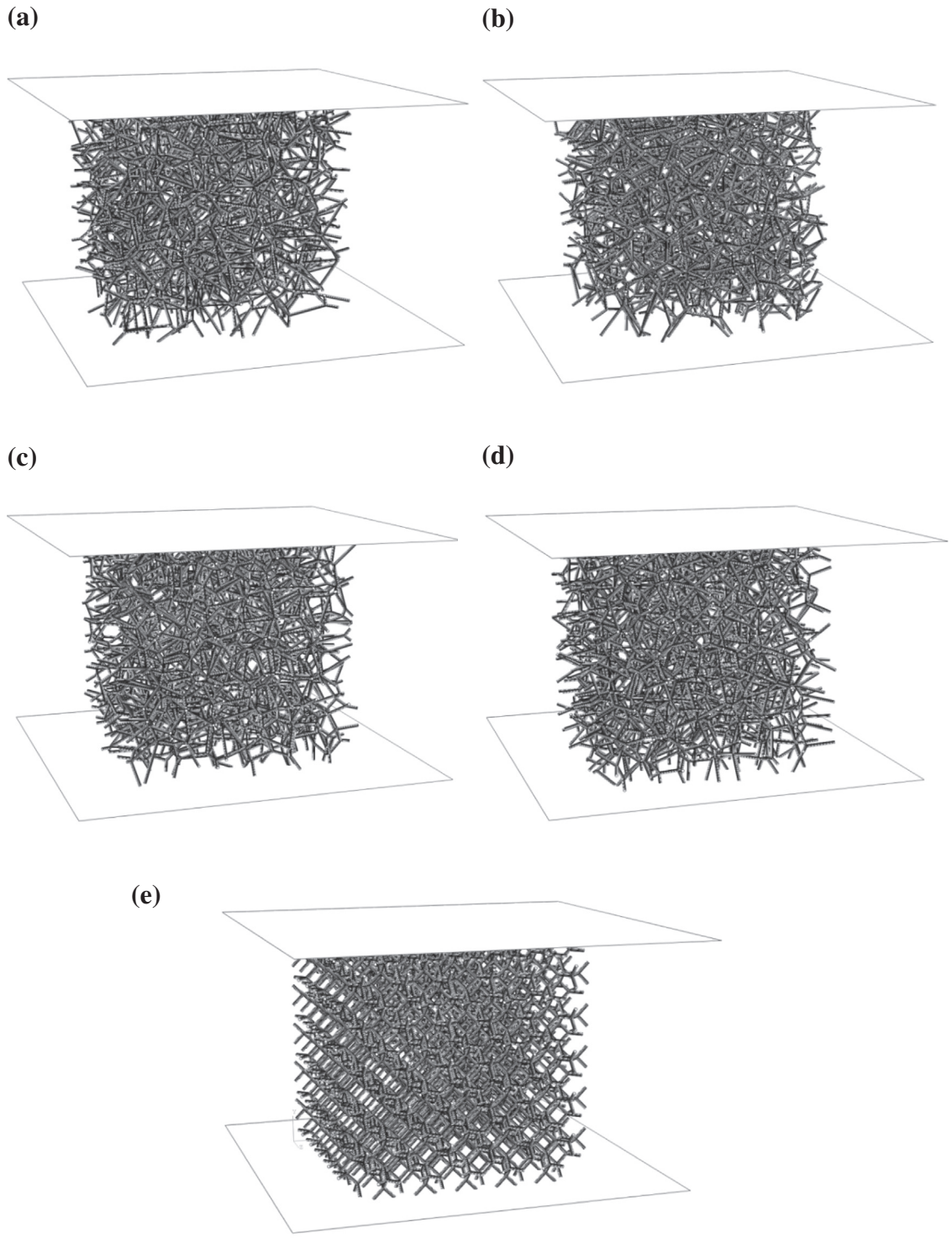

Fig. 2. Solid model geometries of 3-D Voronoi foams for relative density ($\bar{\rho}$) = 3% and different cell regularity δ: (a) δ = 0, (b) δ = 0.5, (c) δ = 0.7, (d) δ = 0.8, (e) δ = 1.

for, say, $n = 341$ nuclei in a 3-D space. A value of $\delta = 1$ implies a regular arrangement of points in a body-centered packing (see Fig. 2e), whereas a regularity parameter of $\delta = 0$ represents a completely random arrangement of points (see Fig. 2a).

Under the assumption that a certain number of nuclei can be generated in a spatial region while maintaining a minimum distance of inhibition, the computational time required for the SSI process to generate nuclei varies depending on the number of nuclei to be generated, the regularity parameter and computational resources available. While it may take only a few seconds to generate a fully random arrangement of nuclei ($\delta = 0$), the computational time required for a random process (SSI) to generate a

regular output ($\delta = 1$) is theoretically infinite according to the probability theory for large numbers (see [6]). To circumvent this problem, in this work, the nuclei of the regular arrangement of points in 3-D were directly located in regular positions of the control volume using the r value without resorting to random generation of points.

2.3. 3-D geometries

While Matlab® was used for dividing space in accordance with the Voronoi tessellation technique, AutoCAD was employed for constructing geometries in 3-D. Four characteristics, namely (i) size of the model (or the number of cells of the foam), (ii) regularity, (iii) cross-sectional shape, and (iv) relative density, were defined for generating spatially monodisperse Voronoi geometries. First, the size of the model that is sufficiently large was considered to represent continuum foam while keeping the size of the model small enough to be manageable with solid modeling and FE computational software packages. Andrews et al. [1] have experimentally studied the effect of the specimen size on the compression response of aluminum foams. They suggest that a ratio of the specimen size to cell size equal to ~6 accurately predicts the elastic modulus and presents a tolerable difference in the prediction of the plastic-collapse strength of aluminum foams. For a regular foam, a ratio of the specimen size to the cell size of 6 corresponds to $n = 341$ cells. Hence, $n = 341$ cells was used to generated 3-D Voronoi foams with a regularity parameter $\delta = \{0, 0.5, 0.7, 0.8 \text{ and } 1\}$. Second, the cross-sectional shape of the struts was modeled as a constant circular cross-section whose area is related to the relative density [41] as:

$$\bar{\rho} = \left(\frac{1}{V}\right)\sum_{i=1}^{N} A_i l_i, \tag{3}$$

where A_i is the cross-sectional area of the struts, $\bar{\rho}$ is the relative density of the foam, N is the number of struts in the cell, h_i is the thickness of struts, l_i is the cell wall length and V is the control volume. Thus, geometries with $\delta = \{0, 0.5, 0.7, 0.8 \text{ and } 1\}$ and relative density $\bar{\rho} = \{3\%, 5\%, 7\% \text{ and } 9\%\}$ were generated. Additionally, plates of thickness equal to ~1% of the sample size were added to the top and bottom of the sample to simulate sandwich structural configurations and prevent unruly local deformations at the top and bottom surfaces when loads were imposed. Examples of the geometries generated for the case of $\bar{\rho} = 3\%$ are shown in Fig. 2. As can be seen in Fig. 2e, the Voronoi configuration for the case of $\delta = 1$ corresponds to a regular arrangement of plane-faced isotropic tetrakaidecahedra.

3. Finite-element modeling

Structural analysis of the foam models was performed using the finite-element package Abaqus/Standard. In the pre-processing stage, the geometries described in Section 2.3 were imported from AutoCAD to Abaqus® as *.iges files. The base material for foam ligaments and face-sheets was modeled as an elastoplastic material with a bilinear isotropic hardening response representative of Al-6101-T6. Specifically, the elastic region was described with an elastic modulus of 68.9 GPa and a Poisson's ratio of 0.33, whereas the plastic region was assigned an initial yield stress of 193 MPa and a slope of $\Delta\sigma/\Delta\varepsilon = 149$ MPa up to a strain of 19%. Beyond that strain the response was assumed constant at 221 MPa.[3] Interactions among the ligaments were seen to occur around 10% strain. Since interaction between beams cannot be automatically simulated in Abaqus/Standard, a high degree of confidence in the results is claimed up to ~10% strain. Nonlinear effects due to large deformations were activated in a general quasi-static analysis performed in Abaqus/Standard. Moreover, convergence issues of an unstable nonlinear problem was improved using an adaptive automatic stabilization scheme [17,20]. Values of 2×10^{-4} and 0.05 for dissipated energy fraction and ratio of stabilization energy to strain energy, respectively, were used in this work.

Equal and opposite displacement boundary conditions were applied to the top and bottom surfaces of the model. Additionally, one point at the center of the top and bottom planes was restrained for translation in the plane perpendicular to the applied displacement direction. The model was discretized with spatial beam elements (B32 in Abaqus) with six degrees of freedom per node (three translations and three rotations) and a quadratic interpolation within the domain of the element. Typically, five nodes per ligament were generated during discretization. Additionally, the top and bottom plates were discretized with four-node shell elements such that nodes in the beams coincide with those of the shell elements. The number of elements in a typical simulation was in the range of 11,114 to 11,860 and more than 50,000 degrees of freedom.

In the post-processing stage, the reaction forces at the bottom surface were added in order to obtain the net reaction force (F). The apparent stress over the Voronoi foam was calculated by dividing F by the area of the base [34]. The average strain was calculated by dividing the displacement over the original length. All these calculations were accomplished for every load increment to produce continuous response curves.

4. 3-D Voronoi foam results

In this section the compression response of Voronoi foams is analyzed. Simulations have been performed for foams with regularities $\delta = \{0, 0.5, 0.7, 0.8, 1\}$ and relative densities of $\bar{\rho} = \{3\%, 5\%, 7\%, \text{and } 9\%\}$ (see Fig. 2 for examples of foam models with $\bar{\rho} = 3\%$) in accordance with

[3] In Appendix A, the elastic properties of face-sheets with a high degree of compliance in the x_1 and x_3 directions are simulated to investigate their influence on the response of the core itself. The effects were found to be negligible. Hence the results can be viewed as the actual response of the foam core itself.

the FE modeling procedure described previously. For the case of $\bar{\rho} = 3\%$, Figs. 3 and 4 superimpose the stress–strain response of Voronoi foams for different regularities. Fig. 3 depicts the response only in the range of 0–0.01 to appreciate the elastic behavior over small strains. The stress has been normalized by the yield stress of the solid material (σ_{ys}) and $\bar{\rho}^{1.5}$. That is, the reduced stress $\bar{\rho}$ is given by:

$$\bar{\sigma} = \frac{\sigma}{\sigma_{ys} \cdot \bar{\rho}^{1.5}}. \tag{4}$$

The quantity $\bar{\rho}^{1.5}$ is used for normalization due to the fact that the foam strength scales with $\bar{\rho}^{1.5}$ as shown later on in Section 4.1. The results presented in Figs. 3 and 4 show that the simulations have been able to capture the two initial regimes (elastic and plateau regions). The elastic modulus shows a direct dependence on regularity. The level

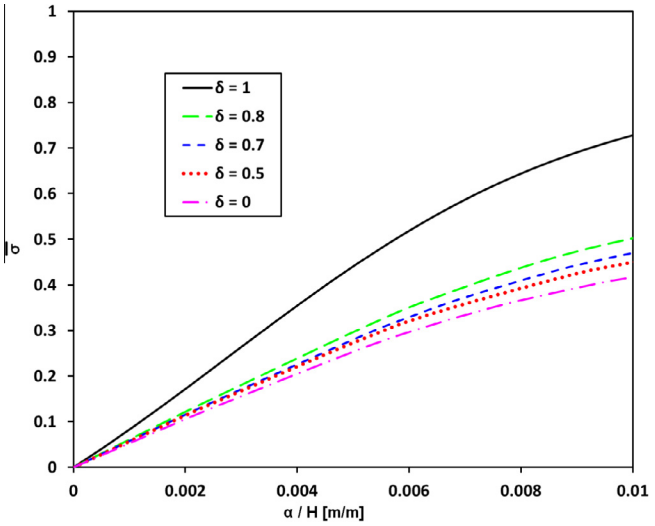

Fig. 3. Normalized stress–strain response of 3-D Voronoi foam with $\bar{\rho} = 3\%$ for different regularities over a strain range of 0–1% (simulated using Al6101-T6 characteristics).

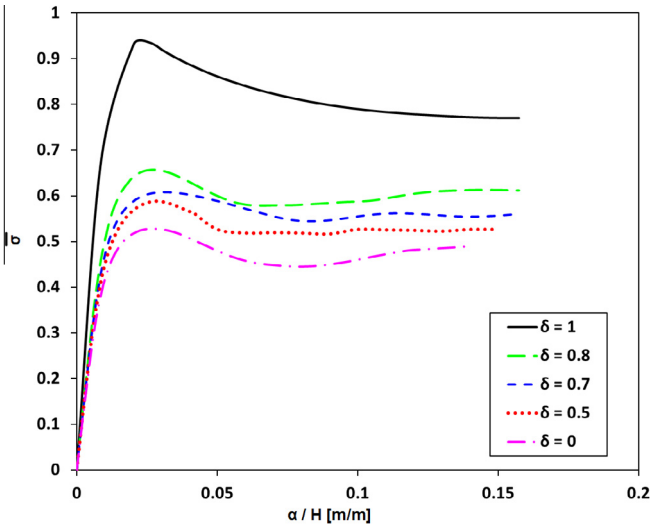

Fig. 4. Response of 3-D Voronoi foams with $\bar{\rho} = 3\%$ for different cell regularities (simulated using Al6101-T6 characteristics).

of variation is quantitatively analyzed in the next section. In the transition zone from elastic to plastic regimes, a drop can be observed after the plastic-collapse strength has been reached. This drop seems to be substantial for the regular configuration ($\delta = 1$) case, when compared to other configuration $0 < \delta < 0.8$, as shown in Fig. 4. Comparable responses such as the ones shown in Figs. 3 and 4 have also been observed for the remaining relative densities $\bar{\rho} = \{5\%, 7\%, 9\%\}$ but are not presented here for brevity. Thus obtained results are, however, analyzed in Sections 4.1 and 4.2.

The deformed foam configuration for the case of $\bar{\rho} = 3\%$ and $\delta = 0.7$ is presented in Fig. 5 for four levels of applied strain. The von Mises stress contours are shown in the same figure. Evidently, the deformation is relatively uniform in the elastic range. The ligaments with higher levels of stress are randomly but uniformly located within the domain of the Voronoi foam. As expected, struts with low levels of von Mises stress are located along the free boundaries of the control volume. (Even though some ligaments with relatively low levels of stress appear to be located within the control volume, in reality, these are located along the free boundary in front of the viewing direction in Fig. 5.) As the imposed displacements increase, deformation starts to localize along a horizontal surface near the center of the control volume although its location can vary due to the random cellular morphology of the foam structure (see Fig. 5d). A similar sequence of deformations and stress–strain responses has been observed for the rest of configurations studied and are not shown here for the sake of brevity.

4.1. The effect of relative density

As shown below, the influence of the face-sheets in the simulations is marginal (see Appendix). Hence, simulations performed in the present study are compared with pure foam models currently available in literature.

Due to the fact that density is one of the parameters that can be controlled during foam production, semi-empirical and analytical studies on the effect of relative density on the elastic response of structural foams are reported in the literature [11,38,43]. First, for low-density foams, Gibson and Ashby [11] used bending theory and a cubic representative volume to derive the general dependency of the elastic modulus with respect to relative density. The relation they proposed is of the form:

$$\frac{E^*}{E_s} = K1\left(\frac{\rho^*}{\rho_s}\right)^2. \tag{5}$$

Additionally, they used experimental data on structural foams in order to extract the value of the constant $K1$. For open-cell configurations, they estimated $K1 \approx 1$. Second, Zhu et al. [43] used a regular tetrakaidecahedron idealization to derive an expression for the elastic modulus of open-cell foams. In case of foams with circular cross-section ligaments like the ones simulated in the present work, the expression is:

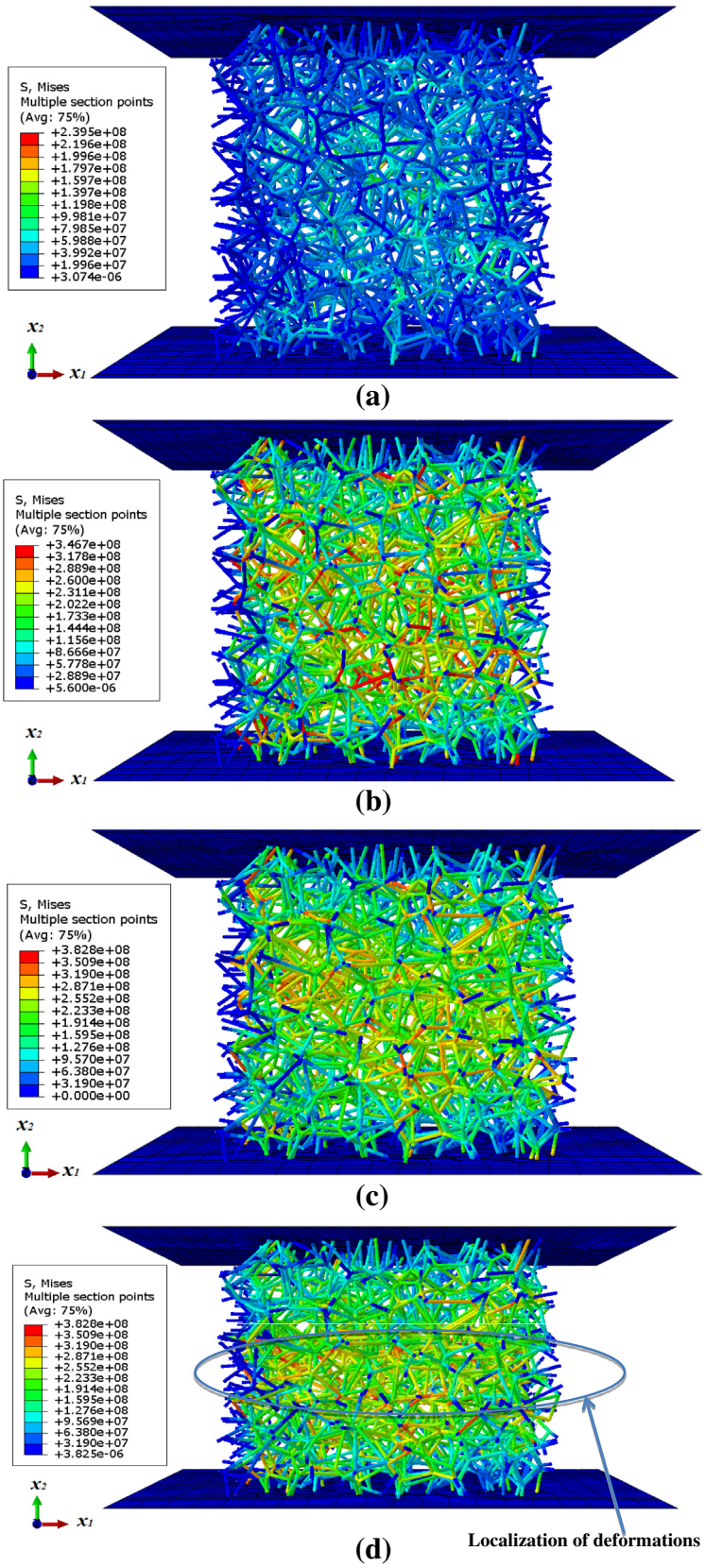

Fig. 5. Von Mises stress contour of aluminum Voronoi foam with $\delta = 0.7$ and $\bar{\rho} = 3\%$ for applied strains of: (a) 1.35%, (b) 2.05%, (c) 8.01%, (d) 15.75%. (Units of stress in the color bar are in Pa.) (For interpretation of the references to colour in this figure legend, the reader is referred to the web version of this article.)

$$\frac{E^*}{E_s} = \frac{3}{5}\frac{\left(\frac{\rho^*}{\rho_s}\right)^2}{\left(1+0.9\frac{\rho^*}{\rho_s}\right)}. \quad (6)$$

Another model for estimating the elastic properties of open-cell foams has been proposed by Warren and Kraynik [38]. In their approach a unit structure formed by struts joining the centroid of a tetrahedron with its vertices was used in order to maintain the 109.5° edge connectivity. Their expression for estimating the elastic modulus is:

$$\frac{E^*}{E_s} = \frac{K2\cdot\bar{\rho}^2(11+4\cdot K2\cdot\bar{\rho})}{10+31\cdot K2\cdot\bar{\rho}+4\cdot K2^2\cdot\bar{\rho}^2} \quad (7)$$

with $\bar{\rho} = \rho^*/\rho_s$ and $K2 \approx 0.827$ for the case of circular cross-section of ligaments.

These analytical and semi-empirical models, along with the current simulations, are comparatively examined in Fig. 6. The results are approximately bounded by those of the Zhu et al. and Gibson et al. models although Zhu et al.'s model is consistently more conservative relative to the present simulations in the range of densities considered. A good correlation between the Warren et al. model and this work for $\delta = \{0.7 \text{ to } 0.8\}$ is also evident in Fig. 6. This is also consistent with the previously published work by Roberts and Garboczi [32]. The simulation results of the present work can be accurately represented by an equation of the quadratic form:

$$\frac{E^*}{E_s} = C3\left(\frac{\rho^*}{\rho_s}\right)^2 + C4\left(\frac{\rho^*}{\rho_s}\right), \quad (8)$$

where constants $C3$ and $C4$ depend on the level of regularity. The values of constants $C3$ and $C4$ obtained by fitting the results computed from Eq. (8) are listed in Table 1 for the different levels of regularity analyzed in the present work.

The dependency of the elastic modulus on $\bar{\rho}^2$ in Eq. (8) indicates that bending is the primary mechanism of deformation [39] as shown by Gibson and Ashby in the derivation of Eq. (5). However, stretching [8] and torsional deformations of ligaments [40] that are also present in these foams can be described with a more complex relationship between the elastic modulus and relative density such as the one considered.

Table 1
Proportionality coefficients $C3$ and $C4$ obtained by fitting elastic modulus data for Voronoi foams of different regularities.

Regularity	$C3$	$C4$	Coefficient of determination
0	0.4826	0.01308	0.9992
0.5	0.4959	0.01483	0.9991
0.7	0.5682	0.01312	0.9993
0.8	0.5998	0.01370	0.9992
1	0.6392	0.02243	0.9989

Similarly, the numerical simulations of Voronoi foams show that the plastic-collapse strength depends on $(\rho^*/\rho_s)^{1.5}$ as observed experimentally [11,12]. For open-cell configurations with ligaments of circular cross-section, Fig. 7 shows the normalized plastic-collapse strength for different levels of regularity:

$$\frac{\sigma^*_{pcs}}{\sigma_{ys}} = C5\left(\frac{\rho^*}{\rho_s}\right)^{1.5} \quad (9)$$

where $C5$ is the coefficient dependent on the regularity of the foam. Table 2 presents the coefficient $C5$ based on fitting the data with the above equation. Expectedly, the value of $C5$ for regular foam ($\delta = 1$) is close to 1, suggesting the high degree of accuracy of these computations.

4.2. Effect of regularity

The effect of the regularity parameter on the compression response of Voronoi foams is evident in Fig. 8. A stiffening response is observed as the cell regularity increases.

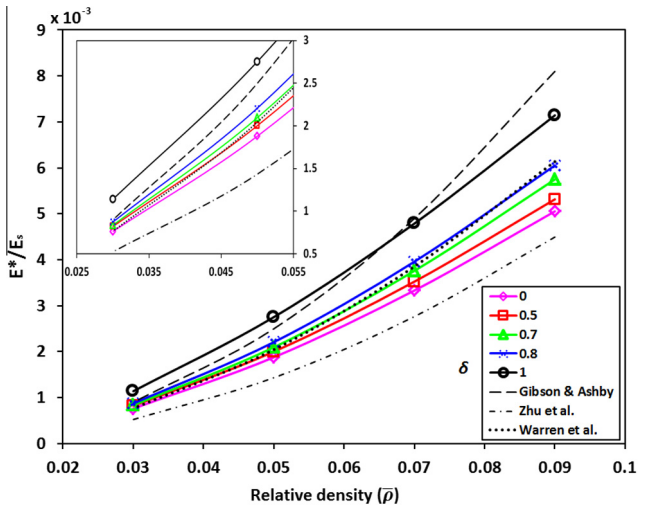

Fig. 6. Variation of elastic modulus of 3-D Voronoi foams with relative density for different cell regularities. Comparison of results with analytical and semi-empirical models. (Inset shows spread of data at low relative densities.)

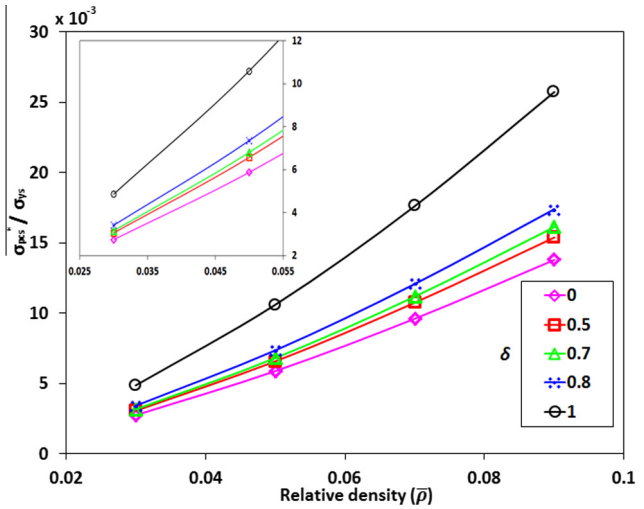

Fig. 7. Effect of relative density on the plastic-collapse strength of different 3-D Voronoi foams. Inset shows enlarged view at small relative densities. (Inset shows spread of data at low relative densities.)

Table 2
Proportionality coefficient $C5$ obtained by fitting plastic-collapse strength for 3-D Voronoi foams of different regularities using Eq. (9).

Regularity	C5	Coefficient of determination
0	0.5150	0.9995
0.5	0.5750	0.9993
0.7	0.6005	0.9998
0.8	0.6482	0.9997
1	0.9516	1

The data suggests that a regular Voronoi foam is {41.3%, 43.7%, 46.5% and 49.5%} stiffer than a fully irregular counterpart for $\bar{\rho} = \{9\%, 7\%, 5\%$ and $3\%\}$, respectively. Previous studies on the elastic compression response of 3-D structural foams were presented by Zhu et al. [41] and Luxner et al. [26]. They, however, come to different conclusions regarding the effect of randomness (or regularity). The current simulations suggest a stiffer response as regularity increases, similar to the conclusion of Luxner et al. However, as noted earlier, this difference could be a direct result of the differences in constructing the geometry.

Fig. 9 shows the effect of regularity on the plastic-collapse strength for different 3-D Voronoi foams. Data indicate an increasing trend in the plastic-collapse strength as the regularity parameter δ increases. Fig. 9 also suggests a sharp rise in the plastic-collapse strength when the regularity is more than $\delta = 0.7$, self-evident for higher relative densities. The strength of a regular tetrakaidecahedron is ~56% higher than that of a foam with a $\delta = 0.7$. Note that the conventional methods of foam fabrication typically produce structural foams with regularities between $\delta = 0.7$ and $\delta = 0.8$. Hence, from the perspective of mechanical response, methods for creating highly regular structural foams are important to pursue since they offer mechanically effective configurations from the perspective of stiffness and yield strength in compression.

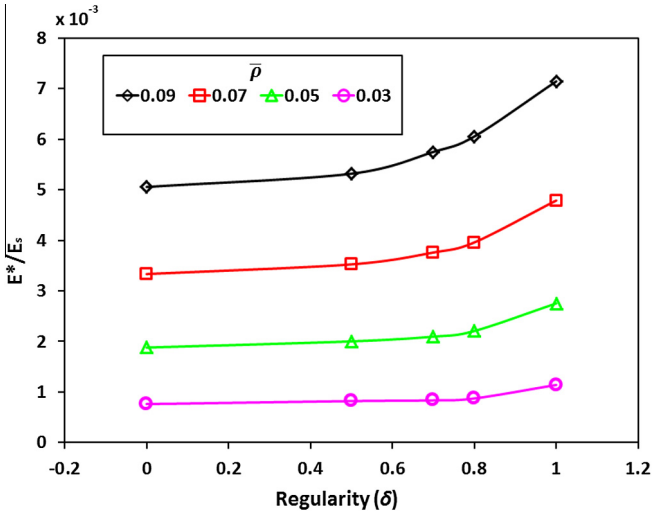

Fig. 8. Effect of cell regularity on elastic modulus of 3-D Voronoi foams of different relative densities.

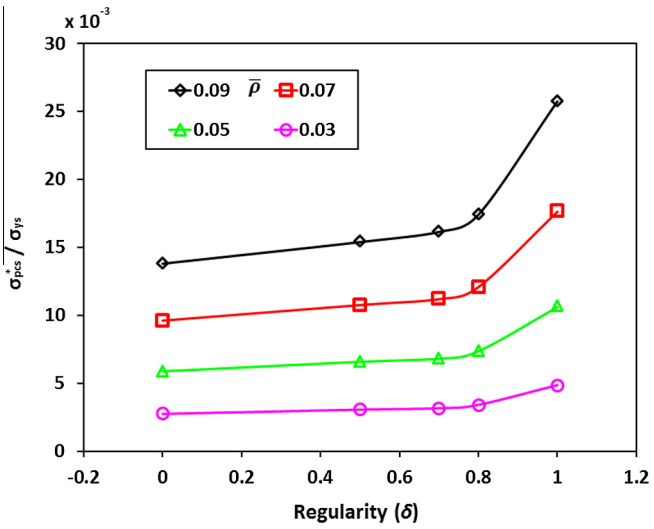

Fig. 9. Effect of regularity on plastic-collapse strength of 3-D Voronoi foams for different relative densities.

4.3. Highly regular 3-D foams

Fig. 9 suggests a relatively steep rise in the mechanical performance in terms of plastic-collapse strength and hence indicates the need for an additional analysis in the range of $\delta = \{0.8$ and $1\}$. That is, analysis needs to be performed on highly regular foams. The previously described SSI process demands huge computational resources in order to generate highly regular foams ($\delta > 0.8$). Hence, highly regular configurations with regularities of $\delta = \{0.8, 0.95$ and $1\}$ were intentionally generated using a perturbation process instead of the SSI process. For this reason, the results for highly regular foams are presented separately to distinguish them from the others generated using the SSI process. In a perturbation process, nuclei were regularly placed in a body-centered arrangement while maintaining a distance among them, calculated using Eq. (1). The Voronoi tessellation technique subsequently generates a regular Voronoi foam (an arrangement of regular tetrakaidecahedra) for the case of a regular arrangement of points $\delta = 1$ (see Fig. 10c). If nuclei are perturbed by adding a random value in the range of $[-h, h]$ to each one of their orthogonal coordinates, the level of regularity can be directly related to the value h for $h \ll r$. Due to the fact that each of the nuclei move to a new random location inside a cube of side $2h$ during perturbation, the minimum possible separation between any two nuclei is:

$$s = r - 2\sqrt{3}h. \tag{10}$$

Thus, the cell regularity, as defined in Section 2.2, is:

$$\delta = 1 - 2\sqrt{3}\frac{h}{r} \tag{11}$$

The required level of regularity can be calculated for a given value of r and h. Conversely, the perturbation introduced is related to the regularity parameter and the maximum possible distance of inhibition r. Recall from the

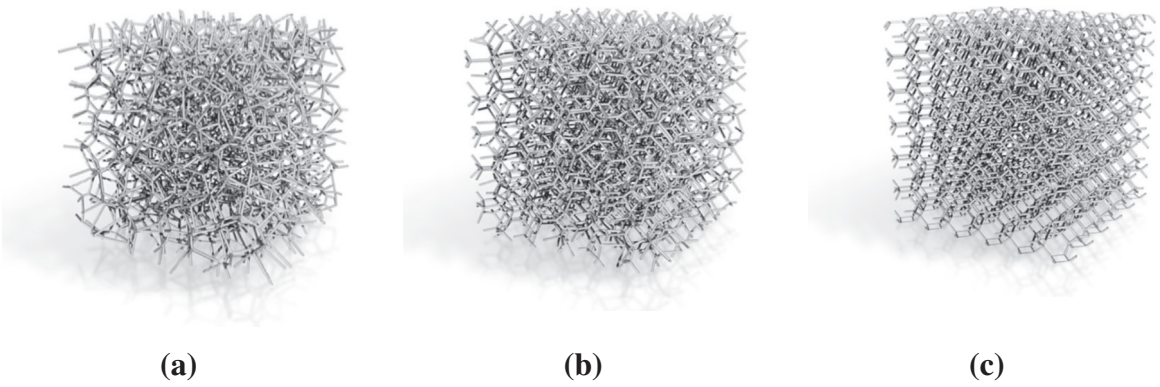

Fig. 10. Computer-generated solid model geometries of highly regular ($\delta > 0.8$) foams using perturbation method, $n = 341$ cells, $\bar{\rho} = 3\%$: (a) $\delta = 0.8$, (b) $\delta = 0.95$, (c) $\delta = 1$.

previous sections that the maximum distance of inhibition is a function of the number of nuclei to be placed in the control volume and the size of the region (space) (see Eq. (1)). Fig. 10 shows the highly regular geometries thus generated for $\delta = \{0.8, 0.95 \text{ and } 1\}$ and $\bar{\rho} = 3\%$. As mentioned earlier, the regular foam was formed by a periodic arrangement of regular tetrakaidecahedron unit cells (Fig. 10). On the other hand, the foams with $\delta = 0.95$ was formed by unit cells that emulate a regular tetrakaidecahedron but perturbed (Fig. 10b). The finite-element procedure explained in Section 3 was followed for highly regular foams also. Fig. 11 shows the stress–strain response for the three geometries presented in Fig. 10. A similar response has been observed for the relative densities $\bar{\rho} = \{9\%, 7\%, 5\%\}$ and are avoided here for brevity. The abrupt softening response observed at yield in regular foams is significantly mitigated by a small perturbation introduced to the foam regularity (from $\delta = 1$ to, say, 0.95). This produces only marginal effects on the elastic modulus and plastic-collapse strength of the foam, as in Fig. 11 for the case of $\delta = 0.95$ without any loss of plateau stress.

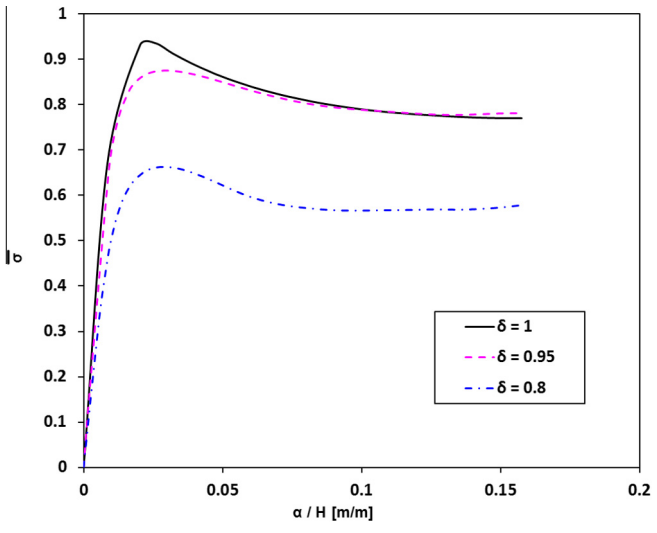

Fig. 11. Normalized compressive stress–strain response of 3-D aluminum Voronoi foams with a $\bar{\rho} = 3\%$ for different highly regular foams.

5. Conclusions

In this paper, the role of cellular morphology of 3-D structural foams on the compression response is studied. Of particular interest to the study is the effect of cell regularity and relative density on the elastic–plastic behavior of random and regular structural foams. Specifically, FE analyses used in conjunction with solid modeling methods have been developed for investigating compression response of foams generated using Voronoi diagrams. The Voronoi tessellation technique in 3-D is applied to represent random foams. The representation captures a majority of characteristics observed in structural foams fabricated using conventional methods, although the surface tension effect which also influence geometry of foams is not accounted for in this work. The advances and accessibility to additive manufacturing methods has motivated this study since Voronoi foams can be directly fabricated from virtual models if they can be numerically developed. This opens the possibility of fully controlling the morphology of structural foams during production in the future. Morphological characteristics such as regularity, cross-sectional shape of ligaments, polydispersity of cells and macroscopic shape that have limited control with conventional methods can be fully defined during virtual design for additive manufacturing purposes.

It is also shown in this paper that the influence of the face-sheets is only marginal. Thus, the results represent the response of 3-D foams itself in view of a relatively large number of cells used in the model. The addition of the face-sheets helps the convergence of the simulation by avoiding premature collapse of struts located at the top and bottom boundaries.

A monotonic direct relationship between the elastic modulus and regularity was identified for Voronoi foams. This observation is consistent with the results reported by Luxner et al. [26] for elastic modulus of 3-D cellular structures consisting of an arrangement of regular tetrakaidecahedra and perturbation of cellular junctions producing random yet nearly regular foams. The current work extends the analysis over the entire range of regularities from $\delta = 0$ to 1. The results suggest that a regular tetrakai-

decahedron foam representation is 41.3%, 43.7%, 46% and 49.5% stiffer than a fully irregular foam for $\bar{\rho} = \{9\%, 7\%, 5\%, 3\%\}$, respectively. The increasing trend in the elastic modulus as the regularity parameter increases was also observed for plastic-collapse strength. The plastic-collapse strength showed a surprisingly sharp rise over the regularity parameter range from 0.7 to 1. The strength of regular tetrakaidecahedron array was ~56% higher than a foam with 0.7 regularity, which is approximately the regularity of structural foams currently fabricated with conventional methods. Thus, the introduction of randomness has a profound effect on reducing the strength of regular 3-D foams in the range from 1 to 0.7. Additionally, the deleterious effect of abrupt softening at yield of regular 3-D foams can be mitigated by introducing a small perturbation to the regularity.

The dependency of the relative density of different Voronoi foam configurations is shown to be bounded by the results of the Gibson and Ashby [11] empirical model and Zhu et al.'s [43] analytical model, although the latter is relatively conservative relative to the FE results of this work. A favorable correlation between the results for the case of Voronoi foams of $\delta = 0.7$ and $\delta = 0.8$ with the Warren and Kraynik [38] model is also observed. A more complex dependency of elastic modulus on the relative density than the one presented by Gibson and Ashby [11] is encountered for 3-D Voronoi foams. Nevertheless, the elastic modulus showed a variation describable by a second-order polynomial and agrees with the results of Gibson and Ashby [11] at the lower range of relative densities considered. On the other hand, the numerical simulations showed that the plastic-collapse strength scales with $\bar{\rho}^{1.5}$, in agreement with the theory of structural foams. However, in the present models the coefficients relating the plastic-collapse strength with relative density vary depending on the regularity parameter of the foam.

Appendix A. Influence of face-sheets

In this paper, face-sheets were added to the top and bottom of the foam geometry in order to prevent premature

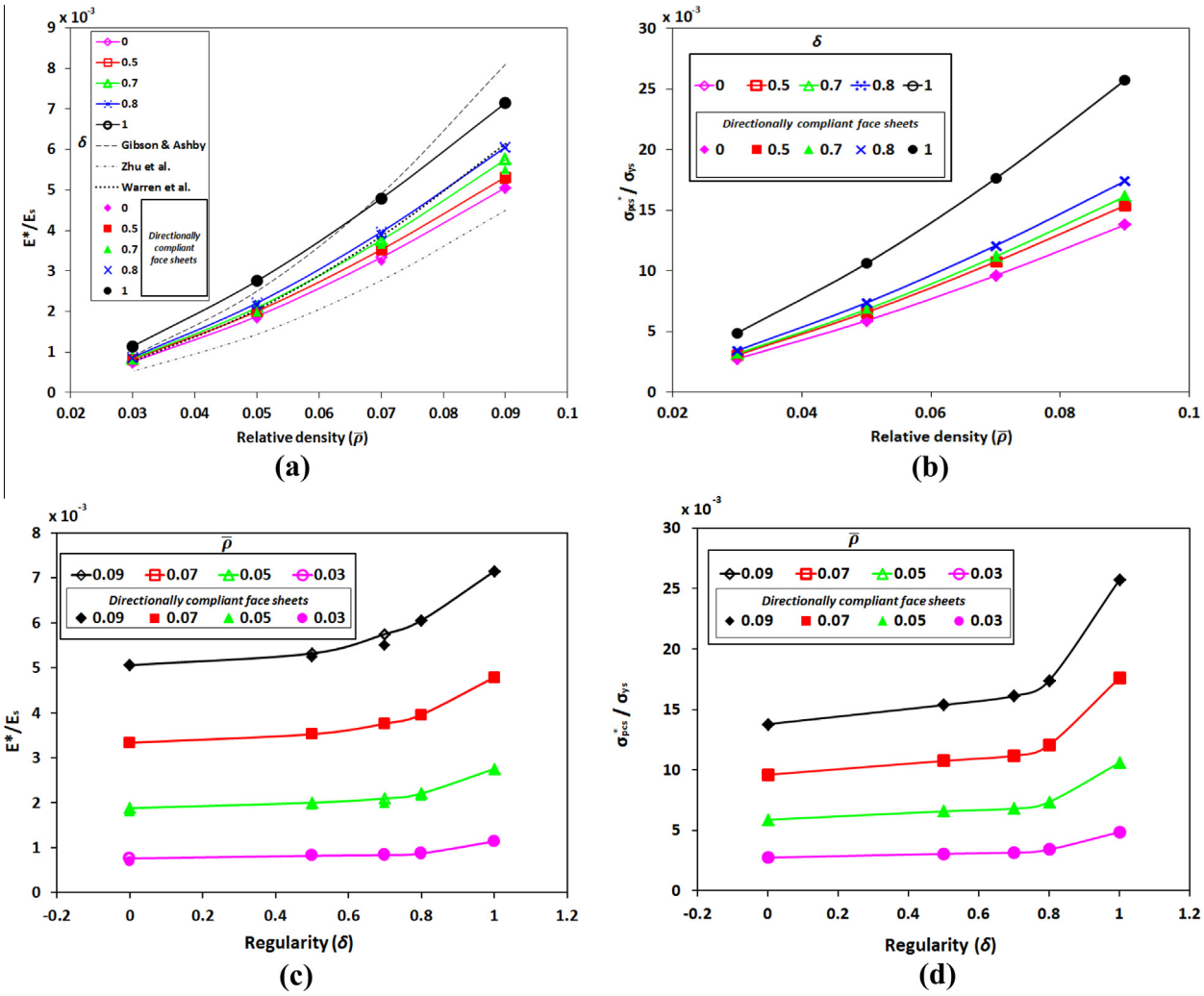

Fig. A1. Results for simulations with directionally compliant face-sheets. The new results (solid symbols) have been plotted along with those from original simulations (open symbols connected by solid lines) shown in (a) Fig. 6, (b) Fig. 7, (c) Fig. 8, (d) Fig. 9. Note that the new results are generally indistinguishable from the earlier simulations, suggesting minimal influence of face-sheets on the results.

collapse of struts due to compression. If the size of the model (or number of cells) is large, the constraining effects (in the x_1–x_3 plane in the present study) of face-sheets on the simulation could be ignored. However, limitation of computational resources sometimes precludes using large models all the time. In such situations, it is of interest to ensure that face-sheets minimally influence the overall response. Accordingly, the number of cells in this paper was increased relative to other studies reported in the literature. Yet, investigating the effect of face-sheet properties on the reported results is appropriate. In the following, compression responses for additional cases, namely orthotropic compliant face-sheet and isotropic compliant face-sheet, are included and compared to the one reported in the main text.

A.1. Directionally compliant face-sheets

Additional simulations were performed on structures described in Section 4. The modification included face-sheets made from orthotropic material with a high degree of compliance in the x_1 and x_3 directions. Specifically, the material of the face-sheets were simulated assuming elastic characteristics, namely $E_{22} = 68.9$ GPa, $E_{11} = E_{33} = 0.2 * E_{22}$, $G_{12} = G_{32} = 25.9$ GPa, $G_{31} = 0.2 * G_{12} = 5.2$ GPa and $v = 0.33$ in all cases. Evidently, the elastic modulus in the direction of compression same as that of the foam ligaments whereas those in the x_1 and x_3 directions were 5-fold lower.

The results of the simulations are presented in Fig. A1. The difference between the simulations with the compliant orthotropic face-sheets relative to the original ones was negligible. That is, the differences on average were 2.4% for elastic modulus and ~0.03% for plastic-collapse strength. This implies that the simulations presented in this work represent actual foam response.

A.2. Isotropic compliant face-sheets

Simulations were repeated with an isotropic compliant material for the face-sheets attached to the foam geometry. The material was idealized to have isotropic elastic properties of $E = 13.8$ GPa and $v = 0.33$. Again, the elastic modulus was assumed to be 5-fold lower than that used in the work described in the paper. The difference between the simulations with the isotropic compliant material for face-sheets relative to the ones in the paper, on average, is ~0.9% for elastic modulus and 1.1% for plastic-collapse strength. Due to such small differences, these results are not presented here for the sake of brevity.

In both the cases, localization of deformations is evident at the center of the model. This sequence of deformation is also similar to the original simulations. In view of these results, one can conclude that the compression characteristics of the Voronoi foam simulated in this work are minimally influenced by the face-sheets. Further, the number of cells is large enough to minimize the influence of displacement constraints in the x_1 and x_3 directions, while preventing premature collapse of foam ligaments and helping improve numerical convergence during simulations.

References

[1] Andrews EW, Gioux G, Onck P, Gibson LJ. Int J Mech Sci 2001;43:701–13.
[2] Ashby MF, Evans A, Fleck NA, Gibson LJ, Hutchinson JW, Wadley HNG. Metal foams: a design guide. Amsterdam: Elsevier; 2000.
[3] Banhart J. Prog Mater Sci 2001;46:559–632.
[4] Barber CB, Dobkin DP, Huhdanpaa HT. ACM Trans Math Softw 1996;22:469–83.
[5] Boots BN. Metallography 1982;15:53–62.
[6] Borel É. J Phys 1913;3:189–96.
[7] Chen C, Fleck NA. J Mech Phys Solids 2002;50:955–77.
[8] Christensen RM. J Mech Phys Solids 1986;34:563–78.
[9] Gaitanaros S, Kyriakides S, Kraynik AM. Int J Solids Struct 2012;49:2733–43.
[10] Gan YX, Chen C, Shen YP. Int J Solids Struct 2005;42:6628–42.
[11] Gibson LJ, Ashby MF. Cellular solids: structures & properties. 2nd ed. Cambridge: Cambridge University Press; 1997.
[12] Gibson LJ, Ashby MF, Harley BA. Cellular material in nature and medicine. New York: Cambridge University Press; 2010.
[13] Gonatas CP, Leigh JS, Yodh AG, Glazier JA, Prause B. Phys Rev Lett 1995;75:573–6.
[14] Gong L, Kyriakides S. Int J Solids Struct 2005;42:1381–99.
[15] Gong L, Kyriakides S, Jang WY. Int J Solids Struct 2005;42:1355–79.
[16] Gong L, Kyriakides S, Triantafyllidis N. J Mech Phys Solids 2005;53:771–94.
[17] K.S. Hibbitt, Inc, 2002. ABAQUSTM User's Manual (version 6.3).
[18] Jang W-Y, Kraynik AM, Kyriakides S. Int J Solids Struct 2008;45:1845–75.
[19] Jang W-Y, Kyriakides S. Int J Solids Struct 2009;46:617–34.
[20] R. Jhaver, Compression response and modeling of interpenetrating phase composites and foam-filled honeycombs (thesis), Mechanical Engineering, Auburn University, 2009.
[21] Kiernan S, Gilchrist MD. Int J Eng Sci 2010;48:1373–86.
[22] Klein R. Concrete and abstract Voronoi diagrams. Berlin: Springer-Verlag; 1989.
[23] Laroussi M, Sab K, Alaoui A. Int J Solids Struct 2002;39:3599–3623.
[24] Lipson H, Kurman M. Fabricated: The New World of 3D Printing. Indianapolis: John Wiley; 2013.
[25] Luxner M, Stampfl J, Pettermann H. J Mater Sci 2005;40:5859–66.
[26] Luxner MH, Stampfl J, Pettermann HE. Int J Solids Struct 2007;44:2990–3003.
[27] Martinez WL, Martinez AR. Computational statistics handbook with MATLAB. London: Chapman & Hall/CRC; 2002.
[28] Moller J. Lectures on random Voronoi tessellations. Berlin: Springer-Verlag; 1994.
[29] Nieh TG, Higashi K, Wadsworth J. Mater Sci Eng: A 2000;283:105–10.
[30] Okabe A, Boots B, Sugihara K, Chiu SN. Spatial tessellations: concepts and applications of Voronoi diagrams. 2nd ed. New York: John Wiley; 1945.
[31] Raj SV. Mater Sci Eng A 2011;528:5289–95.
[32] Roberts AP, Garboczi EJ. J Mech Phys Solids 2002;50:33–55.
[33] Shulmeister V, Van der Burg MWD, Van der Giessen E, Marissen R. Mech Mater 1998;30:125–40.
[34] Silva MJ, Gibson LJ. Int J Mech Sci 1997;39:549–63.
[35] Silva MJ, Hayes WC, Gibson LJ. Int J Mech Sci 1995;37:1161–77.
[36] Tekoglu C, Gibson LJ, Pardoen T, Onck PR. Prog Mater Sci 2011;56:109–38.

[37] Thomson W. Philos Mag Series 5 1887;24(151):503–14.
[38] Warren WE, Kraynik AM. J Appl Mech Trans ASME 1988;55:341–6.
[39] Warren WE, Kraynik AM. J Appl Mech 1997;64:787–94.
[40] Warren WE, Neilsen MK, Kraynik AM. Mech Res Commun 1997;24:667–72.
[41] Zhu HX, Hobdell JR, Windle AH. Acta Mater 2000;48:4893–900.
[42] Zhu HX, Hobdell JR, Windle AH. J Mech Phys Solids 2001;49:857–70.
[43] Zhu HX, Knott JF, Mills NJ. J Mech Phys Solids 1997;45:319–43.
[44] Zhu HX, Thorpe SM, Windle AH. Int J Solids Struct 2006;43:1061–78.